RSC Advances

PAPER

View Article Online
View Journal | View Issue

Cite this: *RSC Adv.*, 2019, **9**, 1726

Influence of magnetic field on electrical and thermal transport in the hole doped ferromagnetic manganite: $La_{0.9}Na_{0.1}MnO_3$

Rajasree Das, Amit Chanda and Ramanathan Mahendiran *

We report the magnetization (M), magnetostriction, electrical resistivity (ρ), thermal conductivity (κ) and thermopower (S) of polycrystalline $La_{0.9}Na_{0.1}MnO_3$ over a wide temperature range of 5 to 360 K. This sample undergoes a paramagnetic to ferromagnetic transition around T_C = 274 K and electrical resistivity ρ shows an insulator–metal transition around T_{IM} = 292 K. The sign of thermopower S is positive in the entire temperature range which indicates that majority charge carriers are holes. Thermopower exhibits a peak and thermal conductivity shows a dip at T_C in the absence of magnetic field. Large difference between the experimentally determined activation energies of ρ and S in the insulating state indicates small polaron hopping dominant conduction above T_{IM}. Polaron formation above T_C, was further confirmed from the anomaly observed in thermal expansion ($\Delta L/L_0$) which shows a change in slope at T_{IM}. In the vicinity of T_C at 3 T applied field, magneto-thermopower (~61.5%) is larger than magnetothermal conductivity (~12.7%) and magnetoresistance (~49%).

Received 20th October 2018
Accepted 7th January 2019

DOI: 10.1039/c8ra08694j

rsc.li/rsc-advances

1. Introduction

Perovskites containing Mn ions (*i.e.* $La_{1-x}A_xMnO_3$, A = Ca^{2+}, Ba^{2+}, Sr^{2+} *etc.*) have been one of the hot areas of research in physics and materials chemistry because of their colossal magnetoresistance (CMR) property and its prospective applications.[1–3] Researchers are intrigued by the rich distinctive physical properties of every member of the manganite-family. From a fundamental point of view, manganites show diverse phenomena such as ferromagnetism, antiferromagnetism, multiferroism, magnetically coupled or independent structural transitions, nano- meso- and micro-scale phase separation, insulator–metal (IM) transition, spin-, charge- and orbital ordering *etc.*[1,4]

$LaMnO_3$ (LMO) containing Mn^{3+} ($t_{2g}^3e_g^1$) cations is a layered A-type antiferromagnetic (AFM) insulator with a Neel temperature (T_N) of 140 K. Substitution with divalent alkaline earth cations (A = Ca^{2+}, Sr^{2+} *etc.*) at the La^{3+} site transforms Mn^{3+} into an equal amount of Mn^{4+} ($t_{2g}^3e_g^0$) and introduces ferromagnetic (FM) spin ordering for x = ~0.18–0.45 in $La_{1-x}A_xMnO_3$.[5] Ferromagnetism and metallic conduction in the divalent ion doped manganites are understood in terms of Zener's double exchange (DE) model.[6] Ferromagnetic metallic state can also be induced by substitution of monovalent cations such as Na^{1+}, K^{1+} or Ag^{1+} for La^{3+} which theoretically should introduce twice the number of holes (or Mn^{4+}) in the structure compared to the same concentration of divalent cation substitution and hence ferromagnetism can be obtained for a smaller amount of Na^{1+} or K^{1+} compared to any divalent ions.

Although thermal transport of hole doped LMO has been investigated in the past few years, the role of magnetic field on the thermal transport of Na^{1+} doped LMO system has been scarcely studied so far. Thermopower (S) is sensitive to band structure and also can probe majority charge carriers. Also S is less affected by the grain boundaries and hence probe intrinsic electrical conduction within grains unlike dc resistivity whose magnitude and temperature dependence is severely modified by grain boundaries. Therefore, S is an effective way to study the transport properties in polycrystalline samples.[7–9] Both Shimura *et al.*[10] and Ahmed *et al.*[11] obtained a negative S in $La_{1-x}A_xMnO_3$ ($x \geq 0.10$) above ferromagnetic transition temperature, but they did not shed light on the trend of thermopower or thermal conductivity under the influence of magnetic field. Studies show that the sign of $S(T)$ can be negative or positive both reflecting holelike or electronlike transport, depending on the temperature and the degree of elemental substitution. 10% Na doping is a critical composition form the point of view that in Ca^{2+} or Sr^{2+} doped compositions S alters the sign with lowering temperature as Mn^{4+} content becomes as high as ~26% (ref. 12) or ~25%,[13] respectively. $La_{0.9}Na_{0.1}MnO_3$ belongs to space group $R\bar{3}c$ like the parent compound with a small decrease in Mn–O bond length and increase in ⟨Mn–O–Mn⟩ angle compared to undoped LMO.[14–16] A doping level exceeding 20% changes the structure from rhombohedral to orthorhombic one.[16] Considering tight-binding approximation for ABO_3 structures, doping

Department of Physics, Faculty of Science, National University of Singapore, 2 Science Drive 3, Singapore – 117542, Republic of Singapore. E-mail: phyrm@nus.edu.sg

Na^{1+} at La^{3+} site affects charge-carrier (e_g electron) bandwidth, $W\left(\propto \frac{\cos\theta}{d_{Mn-O}^{3.5}}\right.$, where $\theta = 180 - \langle Mn–O–Mn\rangle$ and d_{Mn-O} is the Mn–O bond length) advancing DE interaction in the structure.[17] W rises rapidly with a small increase in $\langle Mn–O–Mn\rangle$ angle or decrease in Mn–O length favoring the evolution of the insulator–metal transition[16] which explains the enhancement of T_C by ~150 K in only 10% Na doped LMO.[18]

Recently, nearly 100% suppression of thermopower (negative magneto-thermopower) was reported in antiferromagnetic $Nd_{0.75}Na_{0.25}MnO_3$.[19] An interesting correlation between magneto-thermopower and magnetoresistance was also reported in the same. There has been no report on combined study of thermopower, thermal conductivity and resistivity in Na-doped $LaMnO_3$. In this work, we report simultaneous measurements of the dc electrical resistivity (ρ), thermal conductivity (κ) and thermopower (S) of polycrystalline $La_{0.9}Na_{0.1}MnO_3$ as a function of temperature without and with an external magnetic field. In addition, magnetization, linear thermal expansion and field dependence of magnetostriction are also reported. Our investigation on temperature dependence of magnetization indicates paramagnetic (PM) to ferromagnetic transition at $T_C = 274$ K upon cooling. Magnetic ordering is accompanied by an insulator–metal transition identified by the peak in resistivity curve at $T_{IM} = 292$ K. Thermopower S reveals a hole doping characteristics above and below T_{IM}. The theoretical fitting of $S(T)$ curve indicates that at the FM metallic region, diffusion; phonon drag; magnon drag all coexist whereas at low temperatures (below 80 K), magnon drag dominates the thermopower value. Temperature and field dependent measurements show dominant lattice contribution to the heat conductivity κ.

2. Experimental details

Polycrystalline $La_{0.9}Na_{0.1}MnO_3$ sample was synthesized by solid-state method using high purity La_2O_3, MnO_2 and $NaCO_3$ powders. Stoichiometric amount of the well mixed powders was calcined at 1000 °C for 24 h followed by sintering at 1150 °C for 48 h in few steps of intermediate grinding. The Rietveld refinement of the XRD data reveals the sample belongs to space group $R\bar{3}c$ of the rhombohedral crystal structure. Refined lattice constants of the unit cell are $a = b = 5.5226$ Å; $c = 13.3481$ Å. Magnetization measurements were performed using a Physical Property Measuring System (PPMS), equipped with a vibrating sample magnetometer. The temperature dependence of linear thermal expansion and field dependence of thermal expansion (Joule magnetostriction) were measured using a miniaturized capacitance dilatometer probe designed for PPMS.[20] Four probe dc resistivity, thermopower and thermal conductivity were measured simultaneously at each stabilized temperature using the standard thermal transport option (TTO) for PPMS. In TTO, thermal conductivity (κ) is measured directly from the applied heater power used to create temperature gradient (ΔT) between two ends of the sample. Any heat loss during the measurement is also estimated by the software and the errors due to heat loss is excluded during calculation. However, for thermopower (S) the voltage drop (ΔV) across the hot and cold thermometer probes is also monitored by the TTO system and measured once a stable temperature gradient is created across these two thermometer probes due to the application of heat. PPMS served as a platform to vary temperature and magnetic field. The error for S is almost negligible, whereas, for κ it is <±0.1% at T = 10–100 K and <±5% at higher temperatures. Density of the pellet used for TTO measurement was estimated using Archimedes' principle which was close to 95% of its theoretical value. Magnetoresistance (MR), magnetothermal conduction (MTC) and magneto-thermopower (MTEP) at 3 T magnetic field of the sample is calculated using the standard relations: $\mathrm{MR}(\%) = \frac{\Delta\rho \times 100}{\rho(0)} \equiv [[(\rho(3T) - \rho(0)) \times 100]/\rho(0)]$,

$$\mathrm{MTC}(\%) = \frac{\Delta\kappa \times 100}{\kappa(0)} \equiv [[(\kappa(3T) - \kappa(0) \times 100)]/\kappa(0)]$$

and $\mathrm{MTEP}(\%) = \frac{\Delta S \times 100}{S(0)} \equiv [[(S(3T) - S(0)) \times 100]/S(0)]$,

respectively.

3. Results and discussion

3.1 Magnetic properties

Fig. 1 shows the temperature dependent magnetization (M) of polycrystalline $La_{0.9}Na_{0.1}MnO_3$ (LNMO) sample measured in an applied field of $\mu_0 H = 0.1$ T. The rapid increase of magnetization at $T = T_C$ indicates the onset of ferromagnetism. The ferromagnetic Curie temperature $T_C = 274$ K is determined from the minimum of dM/dT curve as shown in the same figure. The temperature variation of inverse susceptibility ($1/\chi$) and high temperature Curie–Weiss fit, $1/\chi = C/(T - \theta_W)$ of the data points are shown in the inset (a) of Fig. 1. C is the Curie constant given by $C = N\mu_0\mu_B{}^2\mu_{eff}{}^2/3k_B$, where N is the total number of PM entities per cubic meter. Best fitting above T_C in the linear region of $1/\chi$, gives effective moment $\mu_{eff} = 5.98\mu_B$ and Weiss temperature θ_W of 279.3 K which is few kelvin higher than the

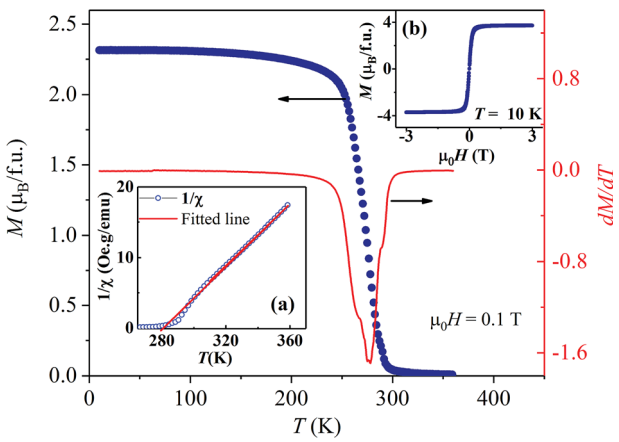

Fig. 1 Temperature dependence of magnetization (M) and dM/dT at an applied field $\mu_0 H = 0.1$ T, inset (a) shows inverse susceptibility *vs.* temperature plot, here solid line represents the Curie–Weiss fitting and (b) shows field dependent magnetization of $La_{0.9}Na_{0.1}MnO_3$ at 10 K.

T_C obtained from M–T curve. The theoretical effective magnetic moment is calculated using the equation, $\mu_{eff} = g\sqrt{S(S+1)}\mu_B$ where, g is the Lande factor and S is the total spin quantum number. In $La_{1-x}Na_xMnO_3$, as we have both Mn^{3+} and Mn^{4+} spin, the modified S will be, $S_{avg} = 2x \times S^{Mn^{4+}} + (1-2x) \times S^{Mn^{3+}}$. As both Mn ions are in the high spin state, *i.e.* $S^{Mn^{4+}} = 3/2$ and $S^{Mn^{3+}} = 2$, the experimentally estimated μ_{eff} is higher than the theoretically expected value of $4.68\mu_B$, considering effective moment of non-interacting Mn^{3+} and Mn^{4+} ions are $4.89\mu_B$ and $3.87\mu_B$, respectively. Enhanced μ_{eff} indicates that spins are not completely independent in the PM state. It is reported that dynamical ferromagnetic nanoclusters do exists in many manganites such as in $(Sm_{0.65}Sr_{0.35})MnO_3$ and $Pr_{0.65}Ca_{0.25}Ba_{0.1}MnO_3$ above T_C.[21,22] Therefore, the above mentioned findings (high values of μ_{eff} and $\theta_W > T_C$) indicate existence of small fraction of ferromagnetic cluster above T_C in LNMO. Inset (b) of Fig. 1 shows field dependence of M at 10 K. It shows soft FM behavior (coercive field = 58.05 Oe) with a maximum moment of $3.7\mu_B$/f.u at 3 T field, which could reach the saturation value of $3.8\mu_B$/f.u expected for 20% Mn^{4+} doped LMO at higher magnetic field. Hence, 10% Na^{1+} substitution dopes nearly 20% of Mn^{4+} in the system.

3.2 Thermal expansion properties

Fig. 2 shows the linear thermal expansion ($\Delta L/L_0$) of LNMO upon cooling from 320 K to 200 K at an external magnetic field of $\mu_0 H = 0$, 1 and 3 T. L_0 is the value of L at 320 K (normalizing temperature), the maximum operating temperature of the capacitance dilatometer. At zero field, $\Delta L/L_0$ decreases with lowering temperature, which indicates a contraction in length of the sample. However, $\Delta L/L_0$ changes slope at the onset of paramagnetic–ferromagnetic transition similar to $La_{0.6}Y_{0.07}Ca_{0.33}MnO_3$.[23] As the external field is applied, the value of $\Delta L/L_0$ decreases around T_C and the change of slope also shifts towards higher temperature because T_C itself increases with increasing strength of the magnetic field. The anomaly in $\Delta L/L_0$ around T_C can be attributed to the localization–delocalization transition of magnetic polarons as in $La_{0.6}Y_{0.07}Ca_{0.33}MnO_3$ (ref. 23) as well as in $La_{0.67}Ca_{0.33}MnO_3$.[24] Magnetic polaron is an entity in which Mn^{3+} (d^4) spins are ferromagnetically aligned locally around a Mn^{4+} (d^3) ions: e_g carrier hops freely within these superparamagnetic clusters. Due to Jahn–Teller nature of Mn^{3+}, lattice distortion also accompanies local spin polarization. Localization of magnetic polarons above T_C causes extra contribution to thermal expansion, which is released when magnetic polarons collapses below T_C leading to decrease in volume. Upon application of magnetic field above T_C, size of magnetic polaron expands and they start percolating which results in enhancement of T_C and shift of the thermal expansion anomaly towards higher temperature. As the magnetic field strength exceeds a critical value, the anomaly is suppressed as the crossover between the low-volume FM and high-volume PM state disappears.

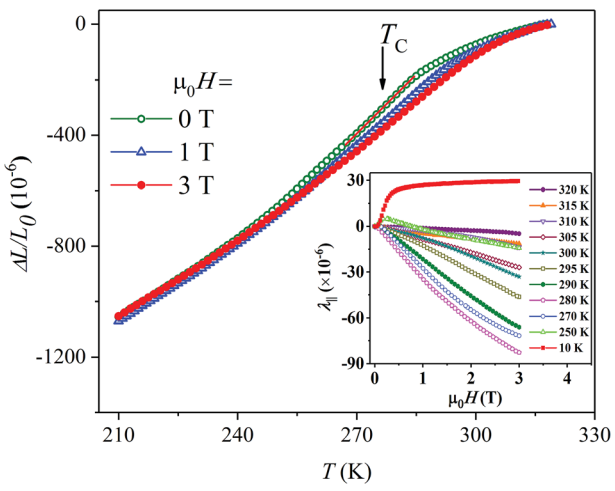

Fig. 2 Temperature dependence of thermal expansion, $\Delta L/L_0$ (normalizing temperature 320 K) at 0, 1 and 3 T applied fields of $La_{0.9}Na_{0.1}MnO_3$ sample. Inset shows magnetostriction, $\lambda_{\parallel}$ (= $[L(H) - L(H=0)]/L_0$) at various temperatures. The measurement uncertainty is about <±3%. The error bar is not shown for purposes of clarity.

The inset of Fig. 2 shows the field dependence of longitudinal magnetostriction *i.e.*, $\lambda_{\parallel}$ (= $[L(H) - L(H=0)]/L_0$) at selected temperatures covering both paramagnetic and ferromagnetic regions. At 10 K, $\lambda_{\parallel}$ increases rapidly in the low magnetic fields and saturates above 0.5 T. However, in the proximity of T_C (250–310 K), $\lambda_{\parallel}$ decreases with increasing strength of the magnetic field and does not show saturation. $\lambda_{\parallel}$ decreases continuously, reaches a minima of -83×10^{-6} near T_C with a subsequent increase for higher temperatures indicating strong spin–lattice and charge–lattice coupling at T_C. The positive magnetostriction at 10 K is caused by increase in length (anisotropic in nature) due to spin–orbit interaction below T_C. However, negative magnetostriction at and above T_C is due to the collapse of magnetic polarons.

The maximum volume magnetostriction is given by $\omega = \lambda_{\parallel} + 2\lambda_{\perp}$, where $\lambda_{\parallel}$ and $\lambda_{\perp}$ are the longitudinal and transverse components of magnetostriction. They are usually measured using strain gauge technique. It was not possible to measure $\lambda_{\perp}$ in our dilatometer probe as it can only measure magnetostriction along field direction, *i.e.* $\lambda_{\parallel}$. In manganites,[23] magnetostriction in the PM state and close to T_C is isotropic, *i.e.*, $\lambda_{\parallel} \sim \lambda_{\perp}$. Therefore, ω near T_C in LNMO can also be expressed as $\omega = 3\lambda_{\parallel}$ which decreases at T_C in zero field.

3.3 Electrical and thermal transport properties

Temperature dependence of the direct-current (DC) resistivity (ρ) at $\mu_0 H = 0$ and 3 T magnetic fields are shown in Fig. 3(a). Upon lowering the temperature, $\rho(T, H = 0\ \text{T})$ initially increases as like a semiconductor and exhibits a sharp peak at $T_{IM} = 292$ K followed by metallic-like behaviour with lowering the temperature further. The insulator–metal (IM) transition temperature T_{IM} *i.e.* the position of resistivity peak is higher than T_C (= 274 K), determined from magnetization measurements, is similar to the report by Ye *et al.*[25] The IM transition temperature is also higher than θ_W (= 279.31 K) estimated from the Curie–Weiss fitting with inverse magnetic susceptibility. Previous reports on similar compounds showed a broad

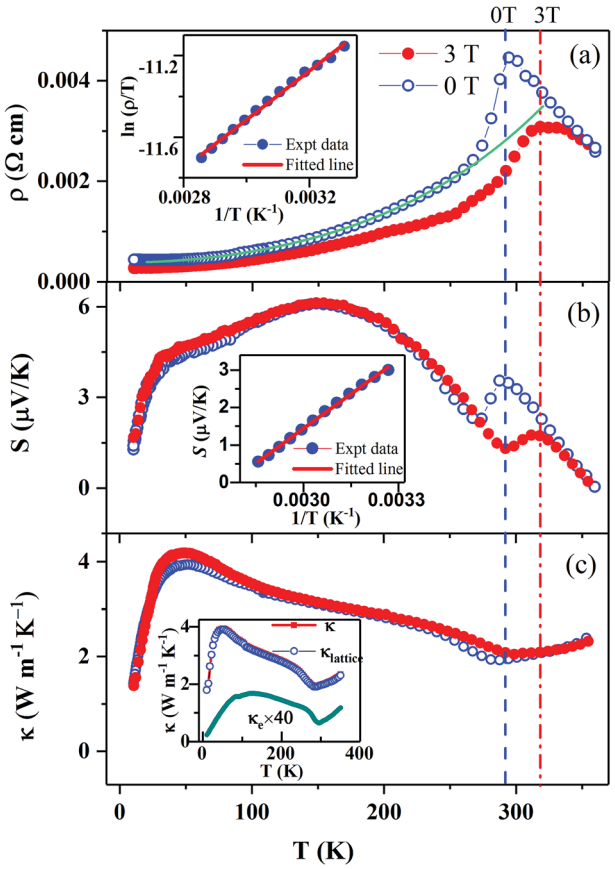

Fig. 3 Variation of (a) resistivity ρ (b) thermoelectric power S and (c) thermal conductivity κ with temperature of $La_{0.9}Na_{0.1}MnO_3$ at zero field (open symbol) and 3 T (closed symbol). The solid curve in (a) is the function $\rho(T) = \rho_0 + AT^2 + BT^{4.5}$. Inset (a) shows $\ln(\rho/T)$ *vs.* $1/T$ plot, and the solid line is obtained by fitting the data according to the small polaron hopping model. Inset (b) includes S *vs.* $1/T$ plot and the solid line is a fitting based on the data. Inset (c) shows plot of κ, κ_e and $\kappa_{lattice}$ *vs.* temperature.

maximum below the resistivity peak due to grain boundaries, those act as regions of enhanced scattering for the conduction electrons and such maximum is absent in our sample.[15,16,18] The peak value of resistivity is reduced and T_{IM} is shifted up under the application of magnetic field.

Fig. 3(b) and (c) show the temperature dependence of thermopower S and thermal conductivity κ, respectively, measured together with dc resistivity. In zero field, sign of S is positive throughout the whole temperature region, which reflects e_g hole of Mn^{4+}: $t_{2g}^3e_g^0$ is the majority charge carrier. Shimura *et al.*[10] obtained a negative S above T_C for $La_{0.88}Na_{0.09}Mn_{0.96}O_3$ and $La_{0.84}Na_{0.12}Mn_{0.97}O_3$ which was attributed to doping induced alteration of conduction from charge transfer type to the Mott-type. In the PM state, $S(T)$ increases with lowering temperature and exhibits a peak at the IM transition and below which it decreases rapidly. However, in the FM state S increases again and shows a broad maximum around 154 K. $S(T)$ shows a striking resemblance with ρ in the presence of an external magnetic field. Applied magnetic field lowers S value prominently in the vicinity of T_{IM} and shifts the peak position to high temperature but it neither influences the value nor the position of the broad maximum at low temperature.

Thermal conductivity (κ) in the paramagnetic state decreases with decreasing temperature (*i.e.* $d\kappa/dT > 0$) which is unusual for a crystalline compound showing insulating like behavior (Fig. 3(c)) but similar to other hole-doped manganites.[26,27] $\kappa(T)$ shows a dip in the vicinity of the magnetic ordering and a few kelvins below the peak in $\rho(T)$ and $S(T)$. Within the FM state below T_C, $\kappa(T)$ increases down to ~43 K, where it reaches a peak and below that κ decreases rapidly. The magnitude of κ in the metallic region varies in the range of 2–4.13 W m^{-1} K^{-1} which is higher than the parent compound (<1 W m^{-1} K^{-1} below room temperature)[28] but comparable with the divalent ion doped systems with similar Mn^{4+} concentration ($\kappa \sim 2.3$ W m^{-1} K^{-1} in $La_{0.8}Ca_{0.2}MnO_3$).[8] The behavior of κ in the paramagnetic region is amorphous like *i.e.*, κ decreases with decreasing T. Such characteristic of κ is attributed to the local anharmonic lattice distortions associated with small polarons or dynamical JT distortion in A-site doped manganites.[26] In general, κ has lattice component $\kappa_{lattice}$ due to phonon vibrations, electronic component κ_e and the spin wave component κ_m, $\kappa = \kappa_{lattice} + \kappa_e + \kappa_m$. Above T_C, κ_m is negligible and the thermal conductivity is primarily due to the other two components. Measured value of ρ is used to calculate κ_e using the Wiedemann–Franz law, expressed by $\kappa_e = L_0T/\rho$, where $L_0 = \pi^2k_B^2/3e^2$ is the Lorentz constant for metals where charge carriers behave like free-electrons (degenerate limit).[29] The estimated κ_e is two orders of magnitude smaller than the total κ in the LNMO sample, which indicates phonon contribution to κ (inset of Fig. 3(c)) is dominant than heat carried by electrical charges. Enhancement of κ on entering the metallic state was argued due to the weakening of JT distortion and delocalization of the charge carriers.[26] The pair distribution function based on the neutron scattering data shows that MnO_6 octahedra in $La_{1-x}Ca_xMnO_3$ (x = 0.2 and 0.25) has uniform Mn–O and O–O bond lengths at low-temperature and when the temperature rises towards IM transition the disorder of Mn–O bond lengths increases followed by the formation of small polarons.[30] Reduction of ρ under magnetic field should have increased κ_e contribution, but in the whole temperature range κ_e value is negligible. A dip in $\kappa(T)$ at T_C or T_N is also seen in other magnetic oxides such as MnO,[31] and it is likely to be caused by decrease in scattering of thermal phonon by spin-fluctuations, which decreases with lowering temperature. The peak at the temperature ~ 43 K is due to transition from umklapp scattering to defect dominated scattering at lower temperatures.

Fig. 4 gives a clear picture of the influence of magnetic field on the physical properties of the system. MR increases with lowering temperature in the paramagnetic state and it reaches a peak value (~49%) at T_C. MR remains significant below T_C and reaches ~40% at 10 K. In the ordered state, ρ rises sharply due to narrowing band width which leads to localization of charges and the formation of small polarons. Application of external magnetic field reduces the relative angle between spins which increases the electron bandwidth and enhances mobility of electrons. In addition to this, destruction of magnetic polarons under applied magnetic field gives rise to a large negative MR.

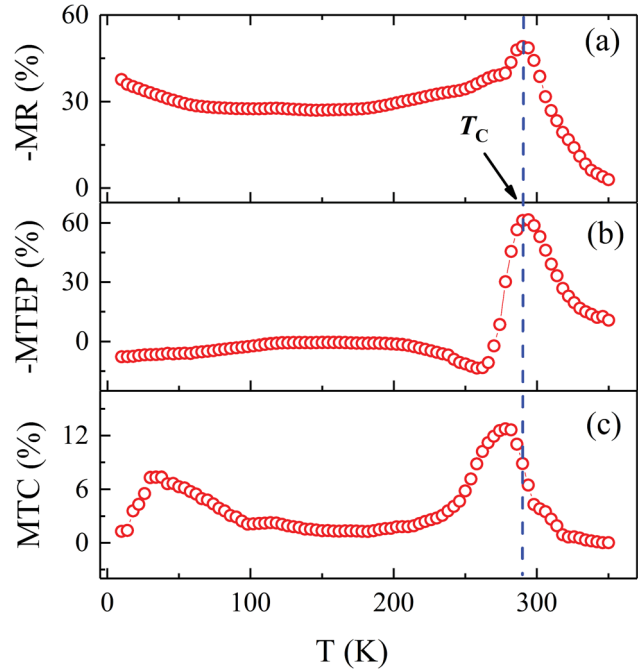

Fig. 4 (a) Plot of magnetoresistance (MR), (b) magneto-thermal conduction (MTC) and (c) magneto-thermopower (MTEP) of $La_{0.9}Na_{0.1}MnO_3$.

For $T \ll T_C$, the magnetoresistance is due to grain boundary effect: tunnelling of spin-polarized electrons between ferromagnetic grains *via* thin grain boundaries.[32] MTEP curve (Fig. 4(b)) reveals very interesting fact that S is affected by the external field mostly around IM transition temperature, whereas S in the FMM region ($T < 260$ K) remains unaffected unlike $\rho(T)$. MTEP is much larger than MR in the temperature interval between T_C (=274 K) and T_{IM} (=292 K) where the spin ordering is destroyed. Unlike MR which is proportional to the density of states (DOS) at the Fermi level, MTEP depends on the asymmetry of DOS around the Fermi level due to the spin-up and spin-down states.[33] Hence, in the FMM state MR is higher than MTEP but as the magnetic ordering collapses MTEP value enhances more than MR. However, MTEP observed here at comparatively low magnetic field (61.5% at 3 T) is comparable with the value (~80–100%) reported for antiferromagnetic $Nd_{0.75}Na_{0.25}MnO_3$ system obtained at 5 T.[19] The magnitude of MTEP of LNMO is also close to the similar amount of hole doped $La_{0.8}Ca_{0.2}MnO_3$ which shows 80% change in thermopower but at 5.7 T magnetic field[8] and single crystal $La_{0.92}Sr_{0.18}MnO_3$ showing MTEP of almost 90% at 7 T.[13] Suppression of S with magnetic field as in LNMO, is observed in few other oxides too.[34,35] Yamamoto *et al.*[34] have shown that in the weakly ferromagnetic $CaRu_{0.8}Sc_{0.2}O_3$ external magnetic field suppresses S, with little influence on ρ. They have also showed a correlation between the spin entropy and magnetothermopower. A similar explanation was also put forward by Repaka *et al.*[36] for the room temperature ferromagnet. In antiferromagnetic $Nd_{0.75}Na_{0.25}MnO_3$, a significant magnetothermopower was found above the Neel temperature even though magnetoresistance was negligible.[19] However in the present study, ρ and S both are significantly affected by the magnetic field around T_{IM} (much above T_C). It appears that S is affected by the change in magnetization to a larger extend than the resistivity. A possible explanation is the decrease in the magnitude of thermopower is partly from the suppression of spin entropy. Another possibility is that the magnetic field affects the spin-dependent band structure around the Fermi level and it is reflected in magnetothermopower as mentioned before. Theoretical modelling is certainly needed to have deeper understanding.

At first sight, thermal conductivity seemed to have very small dependency on external magnetic field (Fig. 3(c)). However, measurement of $\kappa(T)$ in magnetic field makes it easier to understand the influence of spins on the heat transport property of LNMO. Temperature dependence of κ in the hole doped manganites is attributed to two different processes; first one is considered due to the scattering of phonons by Jahn–Teller (JT) distorted $Mn^{3+}O_6$ octahedra[26] and second is to the scattering of phonons by spin fluctuations.[8] At 3 T field, reduction of spin fluctuation facilitates heat flow in the material produces a positive MTC value of about 12.7% near T_C, suggesting spin–phonon scattering as a decisive factor in κ (Fig. 4(c)). Under magnetic field, suppression of the dip in κ around T_C and marginal enhancement in conductivity can be attributed to the scattering of phonons by spin-wave. MR and MTC results unquestionably establish a strong electron–phonon–spin coupling in the Na doped LMO compound.

In manganites, high temperature transport mechanism is often analyzed using fitting of variable-range hopping or small-polaron hopping model with the $\rho(T)$ data. However, in some cases, it is difficult to reach to a satisfactory conclusion based on the fitting results of $\rho(T)$ alone, such as in electron doped $La_{0.9}Te_{0.1}MnO_3$ system[37] which makes it necessary to fit the $S(T)$ data as well. In our sample, high temperature ($T_{IM} \leq T \leq 370$ K) $\rho(T)$ and $S(T)$ data fitted well with the small-polaron hopping (SPH) model, given by

$$\rho(T) = \rho_0 T \exp(E_\rho/k_B T) \quad (1)$$

and

$$S(T) = k_B/e(E_S/k_B T + \alpha), \quad (2)$$

respectively, where ρ_0 and α are constants, k_B is the Boltzmann constant, e is the electron's charge and E_ρ and E_S are the activation energy values obtained from resistivity and thermopower data fitting, respectively (inset of Fig. 3(a) and (b)). We found that E_ρ (103.14 meV) is an order of magnitude higher than E_S (6.13 meV). $E_\rho \gg E_S$ is a hall mark of electrical conduction by small polaron hopping between the neighboring sites.[38,39] E_S corresponds to the hopping energy of carriers between energetically equivalent sites with Fermi level as a reference point for the entropy, while E_ρ contains energy to create the carriers too. Obtained value of E_ρ agrees well with the proper stoichiometric $La_{0.87}Na_{0.13}MnO_3$ compound studied by Malavasi *et al.*[40] Thus, the electrical conduction in LNMO is governed by hopping of small polarons with the energy given by $2(E_\rho - E_S) = 194.02$ meV.[8]

The thermal variation of resistivity below the upturn near T_C (T < 260 K) is dominated by electron–electron scattering (T^2 dependency)[41] and electron–magnon or, spin wave scattering in the ferromagnetic phase ($T^{4.5}$ dependency).[41,42] We have fitted the present experimental data in the FMM phase using an expression of the form, $\rho(T) = \rho_0 + AT^2 + BT^{4.5}$ nearly perfectly as shown by the solid line in Fig. 3(a), where ρ_0 is the residual resistivity due to the temperature independent scattering processes. The fitting parameter A ($\sim 2.17 \times 10^{-8}$ Ω cm K^{-2}) obtained for our samples is similar to that reported by Urushibara *et al.*[41] for La–Sr–Mn–O system and suggests an important role of the electron–electron scattering process below 260 K in the resistivity. Value of B ($\sim 4.73 \times 10^{-15}$ Ω cm K$^{-4.5}$), related to the $T^{4.5}$ behavior suggests that electron–magnon scattering too strongly contributes to the electrical conduction in the FMM region and causes the observed trend in ρ at this temperature range.

The thermopower data in the low temperature metallic region is analyzed using an equation,[37]

$$S = S_0 + S_1T + S_{3/2}T^{3/2} + S_3T^3 + S_4T^4 \quad (3)$$

Here, the first term S_0 is estimated from the high temperature data extrapolation at $T = 0$ K. Second term represents contribution from diffusion, the third term of the equation denotes magnon drag or the single-magnon scattering processes, while the fourth term with T^3 dependency is related to the phonon drag contribution and the last term represents the spin-wave fluctuation in the FM phase below T_C. In general, $S(T)$ of manganites in FM region is analysed without considering the diffusion and phonon drag terms which was quite logical considering the position of low temperature broad peak. Phonon drag peak in thermopower is usually observed near temperature $\theta_D/5$, where Debye temperature θ_D is about 320 K for LMO.[43] Thus, the phonon drag contribution is supposed to show maximum around 60 K much below the observed thermopower peak here at 150 K. To ratify further, LNMO data below $T \ll T_C$ was fitted with equations considering (i) all the terms in eqn (3) and (ii) excluding the diffusion and phonon drag contribution terms in eqn (3). Fig. 5(a) shows a better fitting for the first case throughout a wide temperature range (49–260 K) whereas, the latter one fits the experimental data points only between 150–260 K. Best fitting results ($S_0 = 5.7$ μV K^{-1}, $S_1 = -0.116$ μV K^{-2}, $S_{3/2} = 0.013$ μV K$^{-5/2}$, $S_3 = -2.77 \times 10^{-6}$ μV K^{-4} and $S_4 = 4.06 \times 10^{-9}$ μV K^{-5}) show $S_{3/2} \gg S_3$, suggesting that the electron–magnon scattering strongly affects the broad peak in the S *vs.* T curve but phonon drag is not negligible either. However, in the temperature range below the broad peak (80–30 K) thermopower decreases rapidly showing a $T^{3/2}$ dependence (inset of 4(a)) like in other hole doped manganites.[9,44]

Fig. 5(b) shows the figure of merit ZT, expressed by $ZT = \frac{S^2T}{\kappa\rho}$, a characteristic parameter for the thermoelectric materials. As ZT has a square term of thermopower, it shows a peak around the maxima of $S(T)$. 10% Na doped LMO exhibits better value of ZT compared to $La_{0.9}Te_{0.1}MnO_3$ at room temperature[37] but it is still quite low to be useful for the practical purpose of a thermoelectric material for which $ZT \geq 1$. In the inset of Fig. 5(b), the temperature variation of power factor $\left(\text{P.F.} = \frac{S^2}{\rho}\right)$ is shown. At zero and 3 T applied field, P.F. shows a similar trend with decreasing temperature. It starts increasing rapidly below T_C, goes through a maximum value and then decreases to zero. P.F. has highest value of 0.07 μW cm^{-1} K^{-2} around 47 K at 3 T field.

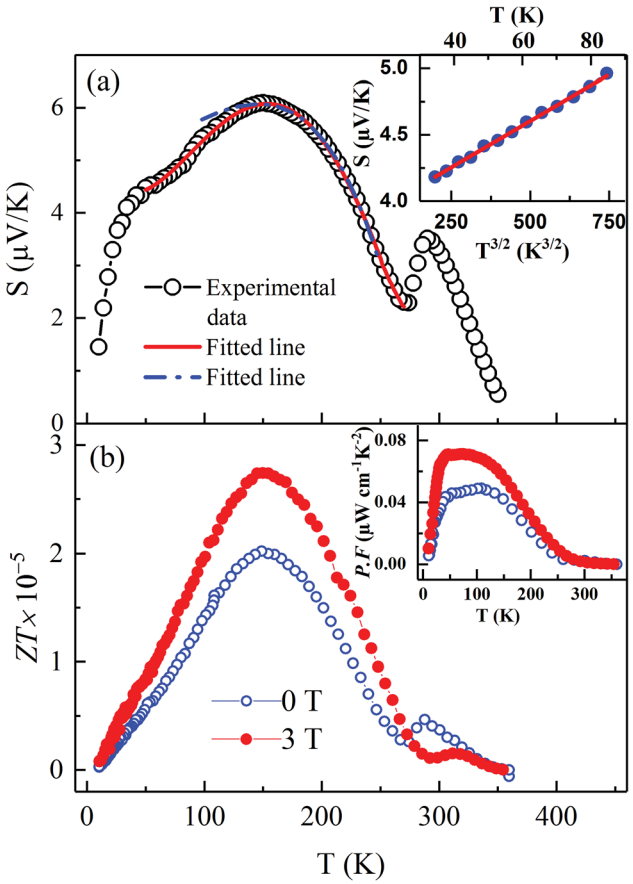

Fig. 5 (a) Temperature dependence of the thermopower for the $La_{0.9}Na_{0.1}MnO_3$ sample. The solid line (red) corresponds to the expression (i) $S = S_0 + S_1T + S_{3/2}T^{3/2} + S_3T^3 + S_4T^4$ and dashed line (blue) represent the fitting with (ii) $S = S_0 + S_{3/2}T^{3/2} + S_4T^4$ as discussed in the text, (b) temperature dependence of figure of merit, ZT for the same sample. Inset of (a) shows $T^{3/2}$ dependency of S at low temperature and (b) power factor (S^2/ρ) at 0 and 3 T fields.

4. Conclusions

To conclude, effects of magnetic field on the thermal expansion, charge transport and thermal conduction mechanism for aliovalent Na^{1+} doped $LaMnO_3$ were investigated. We have found anomaly in thermal expansion behavior around T_C. Electrical resistivity and thermopower data analysis in the insulating region reveal that conductivity at high temperature is governed by small-polaron hopping mechanism in $La_{0.9}Na_{0.1}MnO_3$. Anomaly of κ around paramagnetic–ferromagnetic transition

suggests coupling between thermal conductivity and magnetism. Application of magnetic field enhances thermal conductivity while suppresses the magnitude of thermopower and resistivity. The magnitude of magneto-thermopower (~61.5%) is larger than the magnetoresistance (~49%) and magneto-thermal conductivity (~12.7%).

Conflicts of interest

There are no conflicts to declare.

Acknowledgements

R. M. thanks the Ministry of Education for supporting this work (Grant no. MOE2014-T2-48/R144-000-349-112 and MOE2016-T2-2-098/R144-000-381-112).

References

1 C. N. R. Rao and B. Raveau, *Colossal Magnetoresistance, Charge Ordering, and Related Properties of Manganese Oxides*, World Scientific, Singapore, 1998.

2 J. Hu, L. Shi, Q. Liu, H. Huang and T. Jiao, Improved oxygen reduction activity on silver modified $LaMnO_3$–graphene *via* shortens the conduction path of adsorbed oxygen, *RSC Adv.*, 2015, **5**, 92096.

3 H. Xu, Y. Ma, S. Zhao, W. Huang, Z. Qua and N. Yan, Enhancement of $Ce_{1-x}Sn_xO_2$ support in $LaMnO_3$ for the catalytic oxidation and adsorption of elemental mercury, *RSC Adv.*, 2016, **6**, 63559.

4 Y. Tokura, Critical features of colossal magnetoresistive manganites, *Rep. Prog. Phys.*, 2006, **69**, 797.

5 G. H. Jonker and J. H. Van Santen, Ferromagnetic Compounds of Manganese with Perovskite Structure, *Physica*, 1950, **16**, 337–349.

6 C. Zener, Interaction between the d-Shells in the Transition Metals. II. Ferromagnetic Compounds of Manganese with Perovskite Structure, *Phys. Rev.*, 1951, **82**, 403.

7 A. Bhaskar, M.-S. Huang and C. –J. Liu, Effects of Fe doping on the thermal hysteresis of the $La_{0.5}Ca_{0.5}MnO_3$ system, *RSC Adv.*, 2017, **7**, 11543.

8 B. Chen, A. G. Rojo, C. Uher, H. L. Ju and R. L. Greene, Magnetothermal conductivity of $La_{0.8}Ca_{0.2}MnO_3$, *Phys. Rev. B: Condens. Matter Mater. Phys.*, 1997, **55**, 15471.

9 P. Mandal, Temperature and doping dependence of the thermopower in $LaMnO_3$, *Phys. Rev. B: Condens. Matter Mater. Phys.*, 2000, **61**, 14675.

10 T. Shimura, T. Hayashi, Y. Inaguma and M. Itoh, Magnetic and Electrical Properties of $La_yA_xMn_wO_3$ (A = Na, K, Rb, and Sr) with Perovskite-Type Structure, *J. Solid State Chem.*, 1996, **124**, 250–263.

11 A. M. Ahmed, S. A. Saleh, E. M. M. Ibrahim and H. F. Mohamed, Crystal structure and some transport properties of Na-doped $LaMnO_y$, *J. Magn. Magn. Mater.*, 2006, **301**, 452–457.

12 R. Mahendiran, S. K. Tiwary, A. K. Raychaudhuri, R. Mahesh and C. N. R. Rao, Thermopower and nature of the hole-doped states in $LaMnO_3$ and related systems showing giant magnetoresistance, *Phys. Rev. B: Condens. Matter Mater. Phys.*, 1996, **54**, R9604.

13 A. Asamitsu, Y. Moritomo and Y. Tokura, Thermoelectric effect in $La_{1-x}Sr_xMnO_3$, *Phys. Rev. B: Condens. Matter Mater. Phys.*, 1996, **53**, R2952.

14 M. P. Sharma, *et al.*, Electric transport behaviour of sodium-substituted perovskites $La_{1-x}Na_xMnO_3$ (for $x = 0.1$ and 0.2) and the effect of magnetic fields, *J. Phys.: Condens. Matter*, 2008, **20**, 425220.

15 S. Das and T. K. Dey, Structural and magnetocaloric properties of $La_{1-y}Na_yMnO_3$ compounds prepared by microwave processing, *J. Phys. D: Appl. Phys.*, 2007, **40**, 1855.

16 S. Roy, Y. Q. Guo, S. Venkatesh and N. Ali, Interplay of structure and transport properties of sodium-doped lanthanum manganite, *J. Phys.: Condens. Matter*, 2001, **13**, 9547.

17 P. G. Radaelli, G. Iannone, M. Marezio, H. Y. Hwang, S.-W. Cheong, J. D. Jorgensen and D. N. Argyrion, Structural effects on the magnetic and transport properties of perovskite $A_{1-x}A_x'MnO_3$ ($x = 0.25$, 0.30), *Phys. Rev. B: Condens. Matter Mater. Phys.*, 1997, **56**, 8265.

18 G. H. Rao, J. R. Sun, K. Bärner and N. Hamad, Crystal structure and magnetoresistance of Na doped $LaMnO_3$, *J. Phys.: Condens. Matter*, 1999, **11**, 1523.

19 D. V. Maheswar Repaka and R. Mahendiran, Giant magnetothermopower in charge ordered $Nd_{0.75}Na_{0.25}MnO_3$, *Appl. Phys. Lett.*, 2013, **103**, 162408.

20 R. Küchler, T. Bauer, M. Brando and F. Steglich, A compact and miniaturized high resolution capacitance dilatometer for measuring thermal expansion and magnetostriction, *Rev. Sci. Instrum.*, 2012, **83**, 095102.

21 R. P. Borges, F. Ott, R. M. Thomas, V. Skumryev, J. M. D. Coey, J. I. Arnaudas and L. Ranno, Field-induced transition in the paramagnetic state of $(Sm_{0.65}Sr_{0.35})MnO_3$ associated with magnetic clusters, *Phys. Rev. B: Condens. Matter Mater. Phys.*, 1999, **60**, 12847.

22 A. Mleiki, R. Hanen, H. Rahmouni, N. Guermazi, K. Khirouni, E. K. Hlile and A. Cheikhrouhou, Study of magnetic and electrical properties of $Pr_{0.65}Ca_{0.25}Ba_{0.1}MnO_3$ manganite, *RSC Adv.*, 2018, **8**, 31755.

23 M. R. Ibarra, P. A. Algarabel, C. Marquina, J. Blasco and J. García, Large Magnetovolume Effect in Yttrium Doped La-Ca-Mn-O perovskite, *Phys. Rev. Lett.*, 1995, **75**, 3541.

24 C. Zhu, R. Zheng, J. Su and J. He, Ultrasonic anomalies in $La_{0.67}Ca_{0.33}MnO_3$ near the Curie temperature, *Appl. Phys. Lett.*, 1999, **74**, 3504.

25 S. L. Ye, W. H. Song, J. M. Dai, K. Y. Wang, S. G. Wang, J. J. Du, Y. P. Sun, J. Fang, J. L. Chen and B. J. Gao, Large room-temperature magnetoresistance and phase separation in $La_{1-x}Na_xMnO_3$ with $0.1 \leq x \leq 0.3$, *J. Appl. Phys.*, 2001, **90**, 2943.

26 D. W. Visser, A. P. Ramirez and M. A. Subramanian, Thermal Conductivity of Manganite Perovskites: Colossal Magnetoresistance as a Lattice-Dynamics Transition, *Phys. Rev. Lett.*, 1997, **78**, 3947.

27 A. Ray and T. K. Dey, Thermal conductivity of $La_{0.67}(Ca_xSr_{1-x})_{0.33}MnO_3$ (x = 0, 0.5, 1) and $La_{0.6}Y_{0.07}Ca_{0.33}MnO_3$ pellets between 10 and 300 K, *Solid State Commun.*, 2003, **126**, 147.

28 J. L. Cohn, J. J. Neumeier, C. P. Popoviciu, K. J. McClellan and Th. Leventouri, Local lattice distortions and thermal transport in perovskite manganites, *Phys. Rev. B: Condens. Matter Mater. Phys.*, 1997, **56**, R8495.

29 H.-S. Kim, Z. M. Gibbs, Y. Tang, H. Wang and G. J. Snyder, Characterization of Lorenz number with Seebeck coefficient measurement, *APL Mater.*, 2015, **3**, 041506.

30 S. J. L. Billinge, R. G. DiFrancesco, G. H. Kwei, J. J. Neumeier and J. D. Thompson, Direct Observation of Lattice Polaron Formation in the Local Structure of $La_{1-x}Ca_xMnO_3$, *Phys. Rev. Lett.*, 1996, **77**, 715.

31 G. A. Slack and R. Newman, Thermal Conductivity of MnO and NiO, *Phys. Rev. Lett.*, 1958, **1**, 359.

32 R. Mahesh, R. Mahendiran, A. K. Raychaudhuri and C. N. R. Rao, Effect of particle size on the giant magnetoresistance of $La_{0.7}Ca_{0.3}MnO_3$, *Appl. Phys. Lett.*, 1996, **68**, 2291.

33 M. Czerner, M. Bachmann and C. Heiliger, Spin caloritronics in magnetic tunnel junctions: *ab initio* studies, *Phys. Rev. B: Condens. Matter Mater. Phys.*, 2011, **83**, 132405.

34 T. D. Yamamoto, H. Taniguchi, Y. Yasui, S. Iguchi, T. Sasaki and I. Terasaki, Magneto-thermopower in the Weak Ferromagnetic Oxide $CaRu_{0.8}Sc_{0.2}O_3$: An Experimental Test for the Kelvin Formula in a Magnetic Material, *J. Phys. Soc. Jpn.*, 2017, **86**, 104707.

35 A. Kumar, C. V. Tomy and A. D. Thakur, Magnetothermopower, magnetoresistance and magnetothermal conductivity in $La_{0.95}Sr_{0.05}Co_{1-x}Mn_xO_3$ ($0.00 \leq x \leq 1.00$), *Mater. Res. Express*, 2018, **5**, 086110.

36 D. V. Maheswar Repaka, T. S. Tripathi, M. Aparnadevi and R. Mahendiran, Magnetocaloric effect and magnetothermopower in the room temperature ferromagnet $Pr_{0.6}Sr_{0.4}MnO_3$, *J. Appl. Phys.*, 2012, **112**, 123915.

37 J. Yang, Y. P. Sun, W. H. Song and Y. P. Lee, Thermopower and thermal conductivity of the electron-doped manganite $La_{0.9}Te_{0.1}MnO_3$, *J. Appl. Phys.*, 2006, **100**, 123701.

38 A. J. Millis, P. B. Littlewood and B. I. Shraiman, Double Exchange Alone Does Not Explain the Resistivity of $La_{1-x}Sr_xMnO_3$, *Phys. Rev. Lett.*, 1995, **74**, 5144.

39 M. Jaime, M. B. Salamon, K. Pettit, M. Rubinstein, R. E. Treece, J. S. Horwitz and D. B. Chrisey, Magnetothermopower in $La_{0.67}Ca_{0.33}MnO_3$ thin films, *Appl. Phys. Lett.*, 1996, **68**, 1576.

40 L. Malavasi, M. Cristina Mozzati, P. Ghigna, C. B. Azzoni and G. Flor, Lattice Disorder, Electric Properties, and Magnetic Behavior of $La_{1-x}Na_xMnO_{3+\delta}$ Manganites, *J. Phys. Chem. B*, 2003, **107**, 2500–2505.

41 A. Urushibara, Y. Moritomo, T. Arima, A. Asamitsu, G. Kido and Y. Tokura, Insulator-metal transition and giant magnetoresistance in $La_{1-x}Sr_xMnO_3$, *Phys. Rev. B: Condens. Matter Mater. Phys.*, 1995, **51**, 14103.

42 K. Kubo and N. Ohata, A Quantum Theory of Double Exchange. I, *J. Phys. Soc. Jpn.*, 1972, **33**, 21.

43 B. F. Woodfield, M. L. Wilson and J. M. Byers, Low-Temperature Specific Heat of $La_{1-x}Sr_xMnO_{3+\delta}$, *Phys. Rev. Lett.*, 1997, **78**, 3201.

44 M. Jaime, P. Lin, M. B. Salamon and P. D. Han, Low-temperature electrical transport and double exchange in $La_{0.67}(Pb, Ca)_{0.33}MnO_3$, *Phys. Rev. B: Condens. Matter Mater. Phys.*, 1998, **58**, R5901.